Metal-Ion-Dependent Motion of Self-Propelled Droplets Due to the Marangoni Effect

ARTICLE *in* THE JOURNAL OF PHYSICAL CHEMISTRY B · MAY 2015

Impact Factor: 3.3 · DOI: 10.1021/acs.jpcb.5b02522 · Source: PubMed

2 AUTHORS, INCLUDING:

Takahiko Ban

Osaka University

37 PUBLICATIONS **194** CITATIONS

THE JOURNAL OF PHYSICAL CHEMISTRY B

Article

pubs.acs.org/JPCB

Metal-Ion-Dependent Motion of Self-Propelled Droplets Due to the Marangoni Effect

Takahiko Ban* and Hiroki Nakata

Division of Chemical Engineering, Department of Materials Engineering Science, Graduate School of Engineering Science, Osaka University, Machikaneyama 1-3, Toyonaka, Osaka 560-8531, Japan

Supporting Information

ABSTRACT: Chemically driven self-propulsion of soft matter is useful for various applications because it can move toward a desired location, without external power fields, in response to chemical signals in environmental media. We have developed a suitable steering mechanism to maintain the orientation of self-propelled droplets loaded with surfactant in fluidic environments. A spatial gradient of alkaline-earth metal ions induces directional sensing. These metal ions can be arranged in descending order of directional sensing as $Ba^{2+} \sim Sr^{2+} > Ca^{2+} > Mg^{2+}$. On the other hand, the affinity between metal ions and di-(2-ethylhexyl)phosphoric acid (DEHPA) decreases in the order as $Ca^{2+} > Ba^{2+} > Sr^{2+} > Mg^{2+}$. To clarify the difference between the order of directional sensing and that of affinity, we investigated the effect of metal ions on the driving force to create asymmetric convection. We found that changes in the interfacial tension under nonequilibrium conditions play an important role in directional sensing.

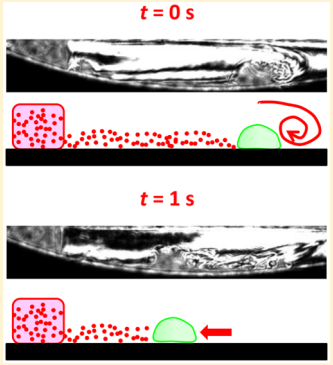

1. INTRODUCTION

In the past two decades, there have been several reports on the spontaneous motion of soft matter arising from a change in the surface energy. Such motion can be experimentally created using thermal,[1,2] electrostatic,[3,4] electrochemical,[5,6] optical,[7,8] and chemical methods.[9−16] There are two types of motions observed in self-propelled soft matter: passive and active motion. Passive motion of soft matter is driven by the prescribed anisotropic fields, and the resulting motion is subject to the gradient of the conservative force.[1−9] Active soft matter moves spontaneously because of the nonlinearity inherent in the system, even in a homogeneous field.[10−16] Nonlinearity in advection coupling with diffusion of chemicals causes a spontaneous breaking in symmetry.[14,16] Passive motion, however, requires external power sources or pretreatment of supported substrates, which could impede practical applications of self-propelled soft matter.

Recently, significant advances have been made in the development of a steering method to maintain the orientation of active matter by the addition of salts. Silver ions changed the propulsion speed of catalytic Janus nanoparticles.[17] The concentration dependence of the speed was exploited for a motion-based nucleic acid detection system.[18] Ebbens et al. reported that the motion of catalytic Janus nanoparticles was due to the combined effects of neutral and ionic diffusiophoretic as well as electrophoresis and that the relationship between these effects could be altered by varying the ionic properties of the fluid.[19] Čejková et al. recently reported that decanol droplets in aqueous solutions of sodium decanoate showed chemotactic movement in response to NaCl concentration gradients.[20] Ban et al. investigated the effect of rare-earth metal ions on the self-propulsion of oil droplets loaded with di-(2-ethylhexyl)phosphoric acid (DEHPA). Self-propelled droplets show directional sensing toward dysprosium ions and extract them autonomously.[21] According to the proposed mechanism of directional sensing, localized dysprosium ions can change the local interfacial tension under nonequilibrium conditions and create an asymmetric convective flow, which can lead to directed motion. However, there is insufficient information on the affinity of DEHPA for rare-earth metal ions, and there is no direct evidence for the statement that dysprosium ions change interfacial tension.

On the other hand, many physicochemical studies have been carried out on the affinity of DEHPA for alkaline-earth metal ions. Static light scattering and Brewster angle microscopy revealed the specific affinity of DEHPA for Ca^{2+} and the presence of macroscopic aggregation.[22,23] Aggregation has an important effect on hydrodynamic instability at the macroscopic scale. A liquid−liquid system of DEHPA in the oil phase and Ca^{2+} in the water phase shows spontaneous fluctuation in interfacial tension, whereas this instability rarely appears in the water phases of Mg^{2+}, Sr^{2+}, or Ba^{2+}. Additionally, a Ca^{2+}-containing pendent droplet formed in the oil phase shows spontaneous and regular oscillation, whereas no oscillation is observed for a droplet of the other metal ions.[24]

In this study, we employed the interaction between alkaline-earth metal ions and DEHPA to steer self-propelled droplets due to changes in the interfacial tension. If these changes occur in a particular region of the droplet interface, they may steer a random convective flow in a certain direction. The resulting

Received: March 16, 2015
Revised: May 21, 2015
Published: May 22, 2015

DOI: 10.1021/acs.jpcb.5b02522
J. Phys. Chem. B 2015, 119, 7100−7105

convective flow can transport the droplet to the desired location. We investigated the effect of various metal ions on the chemotactic behavior of droplet motion. In contrast to our original expectations, the self-propelled droplets showed directional sensing to Sr^{2+} or Ba^{2+}. We measured the interfacial tension between the oil and aqueous phases in the non-equilibrium state in order to clarify the mechanism underlying directional sensing.

2. EXPERIMENT

Nitrobenzene containing 0.1 M DEHPA was used as the oil droplet phase, and phosphate buffer solution (pH 7.41) was used as the aqueous phase. PVA gels containing various alkaline-earth metals ($(MgCl_2(H_2O)_6$, $CaCl_2(H_2O)_2$, $SrCl_2(H_2O)_6$, and $BaCl_2(H_2O)_2)$) were used as the target. Nitrobenzene, phosphate buffer, polyvinyl alcohol, glutaraldehyde, and sulfuric acid were purchased from Wako Pure Chemical Industries. DEHPA was purchased from Sigma-Aldrich. All reagents were used without further purification.

Alkaline-earth metal ions (Mg^{2+}, Ca^{2+}, Sr^{2+}, and Ba^{2+}) were used as chemical signals to steer the self-propelled droplets. In order to localize the alkaline-earth metal ions in the aqueous phase, we prepared a small block of polyvinyl alcohol gel (PVA gel) soaked in solutions containing different metal ions. We used the PVA gel as a pointlike source of chemical signals. The procedure for preparing the PVA gel is described elsewhere.[21] The gel was cut into cubes with their edges 5 mm long and rinsed with pure water in a stirred batch tank several times to remove the acid from the gels until the pH of the rinsing water equaled that of pure water. The resulting gels were soaked in an aqueous solution containing 0.5 M alkaline-earth metal ions. A Petri dish was filled with 10 mL of undiluted phosphate buffer to a height of 3.5 mm. PVA gel containing alkaline-earth metal ions was placed 20 mm from the center of the Petri dish (60 mm inner diameter) and 5 mm from the dish wall. Using a micropipette, an oil droplet containing 0.1 M DEHPA (volume of 3 or 10 μL) was formed at the center of the Petri dish 1 min after setting the gel. The distance between the gel and the 3 μL droplet corresponded to about 15 body lengths (5 body lengths for the 10 μL droplet). The droplet motion was recorded with a high speed camera (Keyence, VW-6000) at a rate of 60 frames per second.

The concentration distributions generated upon the spreading of metallic salt from the gel into the phosphate buffer were recorded with a Mach−Zehnder interferometer (Mizojiri Optical Co., Ltd., MZC-60W). The optical system is illustrated in the Supporting Information. Phosphate buffer solution (4.8 mL) was poured into a rectangular cell ($45 \times 30 \times 50$ mm^3) up to a height of 3.5 mm. PVA gel containing metallic salt was introduced into the cell, and interferograms were recorded using a CCD camera at the rate of 100 frames per second (81 μm/pixel).

The dynamic interfacial tension was measured using a pendent droplet method under nonequilibrium chemical conditions (Dataphysics Instruments, OCA35). A cubic glass cell (20 mm in each dimension) was used as a measuring cell. The cell was filled with 6 mL of buffer solution containing alkaline-earth metal ions at 0.1 mM. The tip of a stainless steel nozzle (1.65 mm and 1.19 mm outer and inner diameters, respectively) was inserted to 7.5 mm below the surface of the solution at the center of the cell. Nitrobenzene solution containing 0.1 M DEHPA was introduced into the nozzle, wherein the supply of the solution was stopped just before droplet detachment. Changes in droplet shape was recorded for 500 s at 30 frames per second. Then, the dynamic interfacial tension was estimated from the droplet shape using the tensiometer software.

3. RESULTS AND DISCUSSION

First, we provide an explanation for the pH-dependent motion of the droplets.[16] The required driving force for such motion is generated by the Marangoni effect due to the deprotonation of DEHPA as the pH in the surrounding medium increases. The deprotonated DEHPA has higher surface activity and causes a decrease in the interfacial tension. The droplets can move spontaneously and sustainably even in a homogeneous pH field, when the initial pH of the continuous phase is adjusted within a range where the interfacial tension decreases significantly in the equilibrium state. The threshold of motility due to the Marangoni effect is determined by the following relation:[14,16]

$$\Gamma_0 M > \frac{3}{2} kR\eta \tag{1}$$

where Γ_0 is the equilibrium surface concentration of the surfactant; $M = d\gamma/d\Gamma$ (γ, interfacial tension), the Marangoni coefficient of the system; k, the rate constant of desorption; R, the droplet radius; and η, a prefactor including the liquid viscosities outside and inside the droplet. When the surfactant supply due to the Marangoni effect exceeds the surfactant consumption through desorption, the resting state becomes unstable, and eventually, the droplet starts to move spontaneously. In this study we defined the term "motility" as spontaneous motion in random directions in the homogeneous concentration field and "directional sensing" as motion-based detection of a gradient of chemoattractant, i.e., to bias motility toward the target by reference to the literature of Swaney et al.[25]

For directional sensing, the droplets need to detect nonuniform distributions of metal ions. Deprotonated DEHPA is accumulated at the interface between nitrobenzene and aqueous phases with the polar headgroup of the deprotonated DEHPA facing the aqueous phase. Thus, the droplets are covered with the negatively charged surfactants, which can serve as a receptor for the metal ions.[21] When the droplets are exposed to a gradient of metal ions, a DEHPA−metal complex is formed at the interface and subsequently desorbed from the interface. This triggers a change in the interfacial tension, creating an asymmetric flow field around the droplets. Directed motion of the droplets is thus induced toward the higher concentration of metal ions. The droplets can thus detect spatial gradients using the interaction between DEHPA and the metal ions.

The salt concentration distribution in the phosphate buffer solution was investigated using a Mach−Zehnder interferometer during salt spreading from the gel. Figure 1 depicts the $MgCl_2$ concentration distribution in the phosphate buffer solution. Spreading of the salt from the lower part of the gel was observed in the horizontal direction. The advancing front of the salt moved at the bottom of the cell. The displacement of the advancing front in the horizontal, x, and vertical, y, directions was measured. The dynamics of the advancing front in the vertical direction indicated a diffusion process (Figure S2). The diffusion coefficient, $D_\perp$, was calculated from $y^2 = 2D_\perp t$ to be 1.0×10^{-9} m^2/s. This value is similar to the diffusion coefficient of Mg^{2+} and Cl^- (0.706×10^{-9} m^2/s and 2.03×10^{-9} m^2/s at 298.15 K, respectively).[26] Figure 2 shows

DOI: 10.1021/acs.jpcb.5b02522
J. Phys. Chem. B 2015, 119, 7100−7105

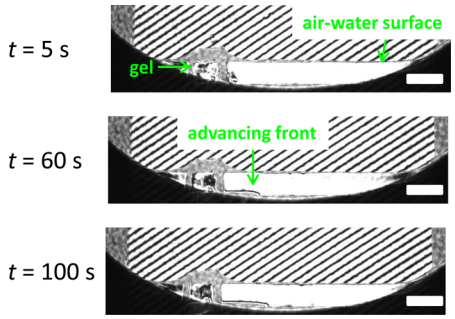

Figure 1. Interferograms during the spreading of $MgCl_2$ from a gel in a phosphate buffer solution. The scale bars are 5 mm.

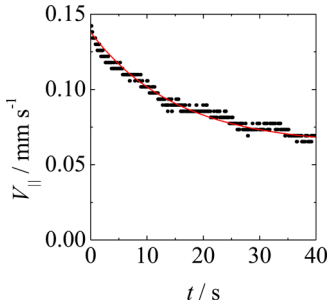

Figure 2. Dynamics of the advancing front of Figure 1 in the horizontal direction. The red curve represents $V_{\parallel} = V_0 e^{-t/\tau} + V_\infty$. The fitting yields $V_0 = 0.075$ mm/s, $\tau = 15.1$ s, $V_\infty = 0.063$ mm/s.

the dynamics of the advancing front in the horizontal direction. The dynamics can be described by the expression $V_{\parallel} = V_0 e^{-t/\tau} + V_\infty$. The salt spreading in the horizontal direction can be regarded as a relaxation process of the solution caused by the density difference between the salt solution contained within the gel and the environmental liquid. In spreading of a heavier liquid in a lighter phase, a horizontal pressure is generated because of hydrostatic pressure.[27] The horizontal pressure decays because of drag. Therefore, the spreading of salt solution was subjected to the relaxation process.

Figure 3 shows interferograms of the chemotactic migration of a self-propelled droplet during $BaCl_2$ spreading from a gel.

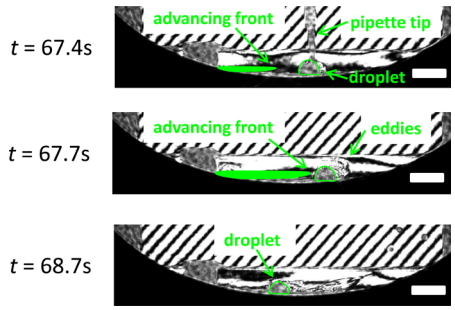

Figure 3. Interferograms during the spreading of $BaCl_2$ from a gel in a phosphate buffer solution in the presence of a 10 μL droplet. The scale bars are 5 mm. The area of spreading salt is filled with a green color. The solid green lines are the periphery of the droplet.

The droplet was formed at a short distance from the advancing front 1 min after setting the gel. Eddies, which were considered as eruption of deprotonated DEHPA, were formed evenly around the droplet just after its formation (see video 1 in Supporting Information). The advancing front suddenly moved toward the droplet. The eddies then decayed on the left side of the droplet, i.e., on the advancing front side. The droplet moved toward the advancing front and eventually reached the gel. This indicated that the metal ions have the ability to direct the fluid flow around a droplet even when the advancing front of the salt does not reach the droplet.

Figure 4 shows 2D trajectories of 3 μL droplets in the presence of a gel containing various metal ions as well as a gel

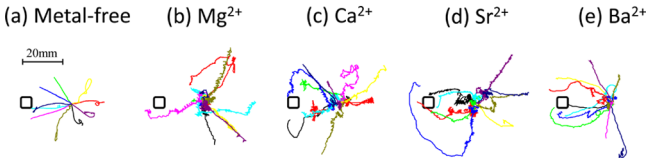

Figure 4. Trajectory for 10 droplets in the case of metal-free situation and in the presence of various metal ions. The black open square represents the gel. The gel was put 20 mm distance away from the droplet.

without metal ions. In the presence of a gel without metal ions, the self-propelled droplets moved in random directions. A few droplets incidentally moved to the gel. On the other hand, for the Sr^{2+} and Ba^{2+} systems, several droplets showed directional sensing to the pointlike source of the target metal ions and moved toward the gel (see video 2 in Supporting Information). These trajectories closely resemble the chemotactic response of cells to the "plane source" of the exponential gradients described in Figure 1B of the literature.[28] Once the droplet approached the gel, a "white cloudlike substance", which was considered to be aggregated metal phosphate, erupted from the gel and moved toward the droplet. The white substance covered the droplet and seemed to pull it nearer the gel. The velocity of the droplet gradually increased as it approached the gel (Figure S4).

Quantitative analysis of the motility of self-propelled droplets requires the use of the mean squared displacement (MSD) from the trajectories.[29,30] We calculated the MSD of self-propelled droplets moving toward the gel containing different metal ions after the intermittent motion. Figure 5 shows the MSD of self-propelled droplets as a function of time. In the presence of a gel containing metal ions, self-propelled droplets show enhancement of the parabolic component of MSD. The propulsion is faster in the presence of a salt gradient. The motion of self-propelled objects at the nanoscale could be caused not by self-propulsion but by spurious effects such as

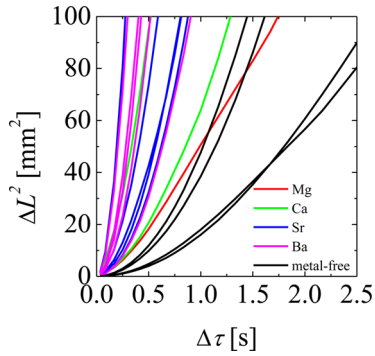

Figure 5. Mean squared displacement as a function of time interval for trajectories of the droplets shown in Figure 4, corresponding to various metal ions.

DOI: 10.1021/acs.jpcb.5b02522
J. Phys. Chem. B 2015, 119, 7100−7105

Table 1. Effect of Metal Ions on the Propulsion Velocity and on the Arrival Rate of 3 μL Droplet[a]

	metal-free	Mg^{2+}	Ca^{2+}	Sr^{2+}	Ba^{2+}
arrival/total	2/10	1/10	3/10	5/10	5/10
V [mm/s]	4.7 ± 1.2	6.3	11.9 ± 6.4	16.5 ± 9.3	21.3 ± 6.8
$\Delta\gamma$ [mN/m]	7.6 ± 0.9	6.0 ± 0.6	4.3 ± 0.9	1.8 ± 0.3	3.0 ± 0.1
γ_c [mN/m]	10.4 ± 0.4	10.6 ± 0.2	6.1 ± 0.1	5.9 ± 0.1	6.0 ± 0.1

[a]The arrival rate is defined as the ratio of the number of self-propelled droplets arriving within a radius 10 mm from the center of a gel to the total number of droplets. The extent of change in interfacial tension and the constant value of interfacial tension under nonequilibrium chemical conditions are summarized in various metal ion systems.

Brownian motion, convection, sedimentation, and contamination.[29] For objects with a radius larger than 500 μm their displacement caused by the Brownian motion is shorter than 0.1 μm for 10 s. We can thus safely ignore the effect of the Brownian motion on the dynamics of self-propelled droplets, since the radius of these droplets is about 800 μm. The experimental results for our system provide clear evidence for the fact that the motility is due to self-propulsion.

Fitting of the MSD yields the motion velocity of self-propelled droplets.[29,30] We could not calculate the chemotactic index used in the literature[28] because the source form of chemoattractant in this study was different from that in the literature. The arrival rate is defined as the ratio of the number of self-propelled droplets arriving within a radius 10 mm from the center of a gel to the total number of droplets. In ballistic motion, ΔL^2 can be fitted by a quadratic curve, $v^2\Delta\tau^2$. The propulsion velocity is calculated from v. Table 1 shows the effect of metal ions on the propulsion velocity and the arrival rate of 3 μL droplets. The velocity represents the average velocity of the droplets moving toward the gel containing the metal ion. The arrival rate in the presence of Ba^{2+} or Sr^{2+} is comparable with the chemotactic index ($\doteqdot$0.3−0.6) of the cells described in the literature.[28] In terms of the arrival rate of self-propelled droplets to the gel the metal ions can be arranged in descending order of directional sensing as $Ba^{2+} \sim Sr^{2+} > Ca^{2+} > Mg^{2+}$. Additionally, Sr^{2+} and Ba^{2+} show a significant increase in propulsion velocity. We confirmed that larger droplets improved the arrival rate. For 10 μL droplets in the Ba system the arrival rate increased up to 70% (7/10). The droplets moved toward the gel without any deviation in direction (see video 3 in Supporting Information). An increase in the area of the droplet surface covered with deprotonated DEHPA may promote sensitivity for detecting the Ba^{2+}concentration gradient. Larger droplets can therefore improve the arrival rate.

Radially symmetric distribution of metal ions from the center of the gel is a reasonable approximation. Then the motion is decomposed into parallel and perpendicular to the radial direction based on the analysis of the trajectories (Table S1). The metal ions can be arranged in descending order of radial velocity as $Ba^{2+} > Sr^{2+} > Ca^{2+} > Mg^{2+}$. This order is consistent with that of directional sensing. The affinity between DEHPA and metal ions, however, decreases in the order $Ca^{2+} > Ba^{2+} > Sr^{2+} > Mg^{2+}$.[22−24] Interestingly, this order is not consistent with that of directional sensing. These results indicate that the metal ions with very low or high affinity have negligible directional sensing effect. Metal ions with medium affinity showed notable sensing. Medium affinity may result in the development of well-defined nonhomogeneous concentration field. The fluid flow around a droplet reacting with metal ion with medium affinity can be reorganized in response to the concentration field. Then, the resulting organized flow can propel the droplet toward the target.

We now discuss the mechanism of chemotactic migration of self-propelled droplets. The left-hand side of eq 1 represents the change in interfacial tension which acts as the driving force. Theoretical studies show that the instability is determined by the product of the Marangoni coefficient and production rate of surface active agents that may change the interfacial tension. The extent of change in interfacial tension with increasing concentration must be positive for increasing the instability to propel the droplets.[14,31] The Marangoni coefficient may be negative if the production rate is negative. In general, however, the Marangoni coefficient is negative in equilibrium because the interfacial tension decreases with an increase in a surface concentration of surfactant. Although the Marangoni coefficient in liquid−liquid systems is negative in equilibrium, systems that show a positive change in the dynamic interfacial tension under nonequilibrium conditions exhibit instability.[32,33] The interfacial tension change under nonequilibrium conditions must act as a driving force to propel the droplets. Therefore, the term $\Gamma_0 M$ in eq 1 should be modified to $(\Delta\Gamma)_{\text{nonequilibrium}}M$, which yields eq 2:

$$(\Delta\gamma)_{\text{nonequilibrium}} > \frac{3}{2}kR\eta \tag{2}$$

To calculate $(\Delta\gamma)_{\text{nonequilibrium}}$ for each system, we measured the time evolution of the interfacial tension of pendant oil droplets containing 0.1 M DEHPA in a phosphate buffer solution with various metal ions.

Typical oscillations in interfacial tension are shown in Figure 6. Interfacial tension in each system suddenly decreased to about 2 mN/m just after the formation of droplets and gradually increased to a constant value after about 100 s. After the induction period, regular oscillations of interfacial tension in each system were observed. A sudden decrease appeared in interfacial tension, and the gradual recovery to a certain constant value was followed by a rapid increase in interfacial

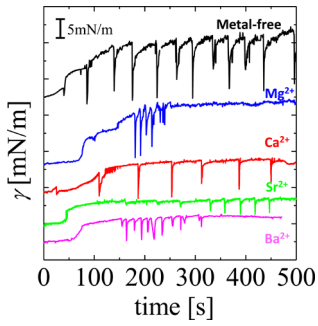

Figure 6. Dynamic interfacial tension of pendent oil droplets containing 0.1 M DEHPA in a phosphate buffer solution with various alkaline-earth metal ions at a concentration of 0.1 mM. The data of interfacial tension are offset for easy comparison.

DOI: 10.1021/acs.jpcb.5b02522
J. Phys. Chem. B 2015, 119, 7100−7105

tension.[16] The sudden decrease in the interfacial tension indicates the formation of a large amount of deprotonated DEHPA at the interface. The increase in interfacial tension, $\Delta\gamma$, indicates a desorption process of the deprotonated DEHPA. The process corresponds to the condition that the Marangoni coefficient is negative when the product rate of deprotonated DEHPA is negative. The extent of change in the dynamic interfacial tension, $\Delta\gamma$, as well as the constant values of the interfacial tension, γ_c, for each system are summarized in Table 1.

For a system without metal ions, the interfacial tension oscillates from 2 to 10 mN/m. The increment in interfacial tension represents the driving force for self-propelled motion and corresponds to the left-hand side of eq 2. The right-hand side of eq 2 is calculated by obtaining the rate constant of desorption, which is $4.2 \times 10^{-3} \pm 2.7 \times 10^{-3}$ mN/m. The calculation procedure is discussed elsewhere.[16] The left-hand side of eq 2 is much greater than the right-hand side. Thus, the droplets in a system without metal ions can move spontaneously even in a homogeneous field.

Directional sensing requires an asymmetric convective flow around the droplets. The asymmetric flow can be generated by an imbalance in the interfacial tension. The interfacial tension depends on the deprotonation of DEHPA. In the previous paper, we showed that the metal ions suppressed the deprotonation of DEHPA using the measurement of the pH change. Therefore, if the metal ions are localized around the droplet, the interfacial tension can be developed inhomogeneously. In the present study we provided the direct evidence that the presence of the metal ions changed the interfacial tension. The induced change in interfacial tension is required for motility. A essential factor for directional sensing is the difference between the extent of change in the interfacial tension in the absence of metal ions and that in the presence of metal ions. Thus, the divalent metal ions with the lower $\Delta\gamma$ can generate more asymmetric flow, which can bias the motility of the droplets toward the gradient of the metal ions. This mechanism is supported by visualization experiments performed on a Mach−Zehnder interferometer. The value of $\Delta\gamma$ for different metal ions follows order $Sr^{2+} < Ba^{2+} < Ca^{2+} < Mg^{2+}$. This order is the reverse of that observed for directional sensing. The metal ions act as "antagonists" that bind to a receptor and suppress the signaling processes.[34,35]

4. CONCLUSION

We investigated the effect of various alkaline-earth metal ions on the motion of self-propelled droplets driven by the Marangoni effect. The droplets showed chemotactic migration with the directional sensing to Ba^{2+} and Sr^{2+}. The ions can be arranged in descending order of directional sensing as $Ba^{2+} \sim Sr^{2+} > Ca^{2+} > Mg^{2+}$. This order is consistent with the suppressing effect of alkaline-earth metal ions on the desorption of DEHPA. This study presents an efficient method for controllable soft matter driven by chemical energy. The ability of self-propelled matter to detect and react to chemical signals can promote its utilization in undertaking tasks too dangerous for humans, in areas where external power sources are not available.

■ ASSOCIATED CONTENT

Supporting Information

Schematic representation of the Mach-Zehnder interferometer, figures of squared displacement of the advancing front, velocity of the advancing front, and relation between velocity and distance, table of effect of metal ions on the velocity, and three movie files that demonstrate various dynamics of chemotactic migration of the self-propelled droplets. The Supporting Information is available free of charge on the ACS Publications website at DOI: 10.1021/acs.jpcb.5b02522.

■ AUTHOR INFORMATION

Corresponding Author

*E-mail: ban@cheng.es.osaka-u.ac.jp. Phone/fax: 81-6-6850-6625.

Notes

The authors declare no competing financial interest.

■ ACKNOWLEDGMENTS

The authors thank Dr. M. Wegener of Henkel for constructive criticisms. This study was supported by the Japan Society for the Promotion of Science (JSPS), Grant-in-Aid for Exploratory Research (Grant 25550069).

■ REFERENCES

(1) Cazabat, A. M.; Heslot, F.; Troian, S. M.; Carles, P. Fingering Instability of Thin Spreading Films Driven by Temperature Gradients. *Nature* **1990**, *346*, 824−826.
(2) Biance, A.-L.; Clanet, C.; Quere, D. Leidenfrost Drops. *Phys. Fluids* **2003**, *15*, 1632−1637.
(3) Washizu, M. Electrostatic Actuation of Liquid Droplets for Microreactor Applications. *IEEE Trans. Ind. Appl.* **1998**, *34*, 732−737.
(4) Pollack, M. G.; Fair, R. B.; Shenderov, A. D. Electrowetting-Based Actuation of Liquid Droplets for Microfluidic Applications. *Appl. Phys. Lett.* **2000**, *77*, 1725−1726.
(5) Phan, C. M. Rechargeable Aqueous Microdroplet. *J. Phys. Chem. Lett.* **2014**, *5*, 1463−1466.
(6) Gallardo, B. S.; Gupta, V. K.; Eagerton, F. D.; Jong, L. I.; Craig, V. S.; Shah, R. R.; Abbott, N. L. Electrochemical Principles of Active Control of Liquids on Submillimeter Scales. *Science* **1999**, *283*, 57−60.
(7) Ichimura, K.; Oh, S.-K.; Nakagawa, M. Light-Driven Motion of Liquids on a Photoresponsive Surface. *Science* **2000**, *288*, 1624−1626.
(8) Berná, J.; Leigh, D. A.; Lubomska, M.; Mendoza, S. M.; Pérez, E. M.; Rudolf, P.; Teobaldi, G.; Zerbetto, F. Macroscopic Transport by Synthetic Molecular Machines. *Nat. Mater.* **2005**, *4*, 704−710.
(9) Chaudhury, M. K.; Whitesides, G. M. How To Make Water Run Uphill. *Science* **1992**, *256*, 1539−1541.
(10) Bain, C. D.; Burnett-Hall, G. D.; Montgomerie, R. R. Rapid Motion of Liquid Drops. *Nature* **1994**, *372*, 414−415.
(11) Yoshikawa, K.; Magome, N. Chemomechanical Transduction in an Oil-Water System. Regulation of the Macroscopic Mechanical Motion. *Bull. Chem. Soc. Jpn.* **1993**, *66*, 3352−3357.
(12) Toyota, T.; Tsuha, H.; Yamada, K.; Takakura, K.; Ikegami, T.; Sugawara, T. Listeria-like Motion of Oil Droplets. *Chem. Lett.* **2006**, *35*, 708−709.
(13) Lagzi, I.; Soh, S.; Wesson, P. J.; Browne, K. P.; Grzybowski, B. A. Maze Solving by Chemotactic Droplets. *J. Am. Chem. Soc.* **2010**, *132*, 1198−1199.
(14) Thutupalli, S.; Seemann, R.; Herminghaus, S. Swarming Behavior of Simple Model Squirmers. *New J. Phys.* **2011**, *13*, 073021.
(15) Nanzai, B.; Ishikawa, R.; Igawa, M. Spontaneous Motion of O-Toluidine Droplets: Repetitive Motion of Running and Squashing. *Chem. Lett.* **2012**, *41*, 609−611.
(16) Ban, T.; Yamagami, T.; Nakata, H.; Okano, Y. pH-Dependent Motion of Self-Propelled Droplets Due to Marangoni Effect at Neutral pH. *Langmuir* **2013**, *29*, 2554−2561.
(17) Kagan, D.; Calvo-Marzal, P.; Balasubramanian, S.; Sattayasamitsathit, S.; Manesh, K. M.; Flechsig, G.-U.; Wang, J. Chemical Sensing Based on Catalytic Nanomotors: Motion-Based Detection of Trace Silver. *J. Am. Chem. Soc.* **2009**, *131*, 12082−12083.

DOI: 10.1021/acs.jpcb.5b02522
J. Phys. Chem. B 2015, 119, 7100−7105

(18) Wu, J.; Balasubramanian, S.; Kagan, D.; Manesh, K. M.; Campuzano, S.; Wang, J. Motion-Based DNA Detection Using Catalytic Nanomotors. *Nat. Commun.* **2010**, *1*, 1−6.
(19) Ebbens, S.; Gregory, D. A.; Dunderdale, G.; Howse, J. R.; Livepool, T. B.; Golestanian, R. Electrokinetic Effects in Catalytic Platinum-Insulator Janus Swimmers. *Europhys. Lett.* **2014**, *106*, 58003.
(20) Čejková, J.; Novák, M.; Štěpánek, F.; Hanczyc, M. M. Dynamics of Chemotactic Droplets in Salt Concentration Gradients. *Langmuir* **2014**, *30*, 11937−11944.
(21) Ban, T.; Tani, K.; Nakata, H.; Okano, Y. Self-Propelled Droplets for Extracting Rare-Earth Metal Ions. *Soft Matter* **2014**, *10*, 6316−6320.
(22) Shioi, A.; Yamada, K.; Shiota, R.; Hase, F.; Ban, T. Chemically Driven Tension Fluctuation and Motion of Interface with Divalent Cation and Di(2-ethylhexyl)phosphoric Acid. *Bull. Chem. Soc. Jpn.* **2006**, *79*, 1696−1703.
(23) Hosohama, T.; Megumi, K.; Terakawa, S.; Nishimura, J.; Iida, Y.; Ban, T.; Shioi, A. Ion-Selective Marangoni Instability Coupled with the Nonlinear Adsorption/Desorption Rate. *Langmuir* **2011**, *27*, 14131−14142.
(24) Ban, T.; Fujii, T.; Kurisaka, K.; Shioi, A. Ionic Control of Droplet Motion. *Chem. Lett.* **2006**, *35*, 1134−1135.
(25) Swaney, K. F.; Huang, C.-H.; Devreotes, P. N. Eukaryotic Chemotaxis: A Network of Signaling Pathways Controls Motility, Directional Sensing, and Polarity. *Annu. Rev. Biophys.* **2010**, *39*, 265−289.
(26) Lide, D. R.; Kehiaian, H. V. *CRC Handbook of Thermophysical and Thermochemical Data*; CRC Press: Boca Raton, FL, 1994.
(27) de Gennes, P.-G.; Brochard-Wyart, F.; Quere, D. *Capillarity and Wetting Phenomena: Drops, Bubbles, Pearls, Waves*; Springer: New York, 2003.
(28) Fuller, D.; Chen, W.; Adler, M.; Groisman, A.; Levine, H.; Rappel, W.; Loomis, W. F. External and Internal Constraints on Eukaryotic Chemotaxis. *Proc. Natl. Acad. Sci. U.S.A.* **2010**, *17*, 9656−9659.
(29) Dunderdale, G.; Ebbens, S.; Fairclough, P.; Howse, J. Importance of Particle Tracking and Calculating the Mean-Squared Displacement in Distinguishing Nanopropulsion from Other Processes. *Langmuir* **2012**, *28*, 10997−11006.
(30) Howse, J. R.; Jones, R. A. L.; Ryan, A. J.; Gough, T.; Vafabakhsh, R.; Golestanian, R. Self-Motile Colloidal Particles: From Directed Propulsion to Random Walk. *Phys. Rev. Lett.* **2007**, *99*, 048102.
(31) Yabunaka, S.; Ohta, T.; Yoshinaga, N. Self-Propelled Motion of a Fluid Droplet under Chemical Reaction. *J. Chem. Phys.* **2012**, *136*, 074904.
(32) Ban, T.; Shioi, A. In *Chemical Reactions on Surfaces*; Dunkan, J. I., Klein, A. B., Eds.; NOVA Science Publishers: New York, 2008; pp 156−194.
(33) Ban, T.; Hatada, Y.; Takahashi, K. Spontaneous Motion of a Droplet Evolved by Resonant Oscillation of a Vortex Pair. *Phys. Rev. E: Stat., Nonlinear, Soft Matter Phys.* **2009**, *79*, 031602.
(34) Artyomov, M. N.; Das, J.; Kardar, M.; Chakraborty, A. K. Purely Stochastic Binary Decisions in Cell Signaling Models without Underlying Deterministic Bistabilities. *Proc. Natl. Acad. Sci. U.S.A.* **2007**, *104*, 18958−18963.
(35) Kolmakov, G. V.; Yashin, V. V.; Levitan, S. P.; Balazs, A. C. Designing Self-Propelled Microcapsules for Pick-Up and Delivery of Microscopic Cargo. *Soft Matter* **2011**, *7*, 3168−3176.

DOI: 10.1021/acs.jpcb.5b02522
J. Phys. Chem. B 2015, 119, 7100−7105